

Near infrared spectroscopy can accurately estimate biodiesel cetane number

Good agreement between NIRS and proposed equations in literature

Near infrared spectroscopy can be used for real-time cetane number determination

1 **Cetane number prediction of waste cooking oil-derived biodiesel prior**
2 **to transesterification reaction using near infrared spectroscopy**

3 Juan Francisco García-Martín*, Francisco Javier Alés-Álvarez, María del Carmen

4 López-Barrera, Irene Martín-Domínguez, Paloma Álvarez-Mateos

5 Departamento de Ingeniería Química, Facultad de Química, Universidad de Sevilla, C/

6 Profesor García González, 1, 41012 Seville, Spain

7 *Corresponding author. E-mail address: jfgarmar@us.es

8

9 **Abstract**

10 Fifty waste cooking oils (WCOs) were transesterified with methanol (1:8
11 WCO:methanol molar ratio) at 60 °C for 60 min using NaOH as catalyst (1 % wt.).
12 Fatty acid methyl ester (FAME) composition of the resulting biodiesels was analysed by
13 gas chromatography, and near infrared (NIR) spectra of these biodiesels and those of the
14 starting WCOs were acquired. Biodiesel cetane number was then calculated from both
15 FAME composition and from biodiesel NIR spectra, this last technique using the former
16 one as reference data. Because of transesterification does not modify fatty acid
17 distribution of the starting WCO, and the similarity between biodiesel and WCO NIR
18 spectra, biodiesel cetane number was successfully predicted from WCO NIR spectra,
19 achieving RPD (ratio of performance to deviation) of 3.83. Therefore, biodiesel cetane
20 number (and, as consequence, any other biodiesel property related to FAME
21 composition) can be predicted by NIR spectroscopy before performing the
22 transesterification reaction, which allows beforehand selecting the most suitable
23 substrates for biodiesel production.

24 Keywords: biodiesel; cetane number; NIRS; waste cooking oil.

25 **1. Introduction**

26 Because of fossil fuels are depleting and the hazardous effects of these fuels on the
27 environment, current researches mainly focus on the search for economic raw materials
28 that can reduce environmental pollution and can be used for the production of efficient
29 substitutes for petroleum fuels. Concerning diesel, its combustion leads to air pollution
30 by greenhouse gases emissions (NO_x , CO, CO_2), and to the destruction of the ozone
31 layer by photochemical interactions of hydrocarbon, CO and NO_x emissions.

32 Due to these drawbacks, an alternative to diesel fuel is required. One of the most
33 attractive and biodegradable alternatives is biodiesel, which is composed of fatty acid
34 methyl esters (FAMES). Biodiesel is obtained by transesterification of vegetable oils
35 with methanol in the presence of a catalyst. Although other short-chain alcohols, such as
36 ethanol, can be used, methanol is usually selected because it is the least expensive
37 alcohol. This reaction normally does not alter fatty acid composition, so the biodiesel
38 fatty acid profile matches with that of the starting oil [1–4]. The use of biodiesel can
39 reduce the global emissions of CO_2 and greenhouse gas particles because the carbon
40 contained in the biofuel is biogenic and renewable. That is, CO_2 enters a closed cycle
41 generated by photosynthesis that helps to reduce the greenhouse effect. Besides,
42 biodiesel can easily decompose under natural conditions (more than 90 % of pure
43 biodiesel can be degraded in a few weeks), and its sulphur content is almost nil [4,5].
44 Furthermore, biodiesel has greater cetane number (an important diesel quality
45 parameter) than petroleum diesel. This improves the combustion efficiency, shortens
46 ignition delay, increases compression ratio of the engine and produces less noise and
47 pollutants (NO_x , CO and hydrocarbons).

48 Cetane number depends on biodiesel fatty acid profile, so several equations that relate
49 cetane number to FAME have been proposed [3,6–11]. Of note is that cetane number
50 depends on both moieties of the fatty acid alkyl ester (the fatty acid and the alcohol), i.e.
51 cetane number of biodiesel from the same oil will differ if the transesterification is
52 carried out with methanol or ethanol. The application of these equations requires the
53 previous determination of FAME composition by gas chromatography, which limits
54 their application due to the cost of this technique.

55 Near-infrared spectroscopy (NIRS) is a low-cost, safe and non-destructive technique
56 which requires minimal or no sample preparation and relatively small amounts of
57 sample for analysis [12]. These features make NIRS suitable for online work. The
58 potential of NIRS for biodiesel analysis, including biodiesel feedstock selecting,
59 transesterification reaction monitoring, and determination of biodiesel blend level,
60 properties and contaminants, has been comprehensively reviewed [13]. It has been
61 verified that FAME composition of oils and biodiesel can be determined by NIRS with
62 great accuracy [14,15]. As cetane number can be calculated from FAME composition,
63 cetane number could be directly calculated from NIR spectra. What is more, since
64 transesterification does not alter fatty acid composition, cetane number could be
65 predicted from FAME composition of the starting oil.

66 The main problem in the production of biodiesel is the cost of the raw material
67 (generally vegetable oils) resulting in biodiesel prices higher than those of petroleum
68 diesel. One way to cut costs is the use of waste cooking oils (WCOs) as raw material.
69 Used oils must be safely disposed in the EU in order to not to be harmful to humans or
70 the environment (Council Directive 75/439/CEE of 16 June 1975). Therefore, the use of
71 WCOs for biodiesel production can be the best economic alternative for the recycling
72 and reutilization of these oils.

73 When an oil is used for frying, it undergoes numerous physical and chemical changes
74 that modify its properties. The most common physical changes in WCOs are increase of
75 viscosity [16,17], decrease of surface tension [18] and changes in sensory attributes
76 [17,18], while the thermal (temperatures above 160 °C), oxidative (through a
77 mechanism of free radicals) and hydrolytic reactions result in the formation of alkanes,
78 alkenes, symmetrical ketones of lower fatty acids, oxopropyl esters, aldehydes,
79 semialdehydes, hydrocarbons, oxidized polymers, free fatty acids, glycerol,
80 monoglycerides and diglycerides [17].

81 High acidity values are a significant hindrance for biodiesel production. If an oil has
82 free fatty acids, the catalyst reacts with them to form soap and water (saponification
83 reaction) with the consequent biodiesel yield decrease and reagent cost increase.

84 The main objective of this paper was to predict the cetane number of a future biodiesel
85 from its starting WCO NIR-spectrum features, which will allow biodiesel
86 manufacturers to select or discard a raw material for biodiesel production without the
87 need to perform first the transesterification reaction. To do this, we first verified that
88 cetane number can be obtained from biodiesel NIR spectrum and afterwards we assayed
89 cetane number prediction from WCO NIR spectrum.

90

91 **2. Material and Methods**

92 2.1. Waste cooking oils (WCOs)

93 Fifty oils used for frying were supplied by the university canteen of the Reina Mercedes
94 Campus (University of Seville) and private households. These WCOs were olive,
95 sunflower and pomace oils, and mixtures of olive and sunflower oils (Table 1). This
96 ensured a wide variety of oil types and frying habits in the WCO samples.

97 2.2. WCO conditioning

98 WCOs were firstly filtered to remove impurities such as leftover food, flour, etc. They
99 may also contain a significant amount of water, however WCOs were not vacuum
100 heated in order to obtain a wider range of biodiesel yields.

101 2.3. Biodiesel production

102 250 g WCO were mixed with 68.5 g methanol (1:8 molar ratio) and placed inside a 0.5-
103 dm³ stirred tank batch reactor together with 1 % (wt. WCO) sodium hydroxide.

104 Transesterification reaction took place at 60 °C for 60 min. Stirring was set to 750 rpm,
105 diameter shovel being 6 cm. The reactor was equipped with a Dimroth condenser to
106 prevent methanol losses.

107 Once the reaction was complete, the reaction mixture was let stand overnight. Two
108 phases were separated, an upper phase of methyl esters in methanol and a lower phase
109 containing about 10 % of the weight of the starting WCO, composed of glycerin and
110 methanol excess. Subsequently, both phases were subjected to rotary evaporation to
111 remove methanol. Finally, biodiesel was filtered using a Büchner funnel with a layer of
112 Eco2Pure adsorbent (heat- treated hardwood shaving combined with crystalline
113 aluminosilicate with binders) supplied by Filbertechnik Ltd. (United Kingdom), thus
114 eliminating moisture and formed soaps from free fatty acids.

115 2.4. Analytical methods

116 2.4.1. Free acidity (FA) analysis

117 Once the WCOs were clean, FA was measured, that is, the percentage of free fatty acids
118 WCOs contain. FA was expressed as oleic acid percentage and analysed according to
119 the Official Methods of Analysis of the EC [19,20]. Briefly, 4–6 g WCO were placed
120 into 250-cm³ wide-mouth Erlenmeyer flask along with 50 cm³ ethyl alcohol:ethyl ether
121 solution (1:1 v/v) and a few drops of phenolphthalein, and then neutralized with 0.1 N
122 NaOH until pink in colour. The FA contents ranged between 0.15 % and 9.73 % (Table

123 1). WCOs with FA higher than 2.5 % were pre-esterified with methanol using 1 % (wt.)
124 sulphuric acid as catalyst in the same reactor and under the same conditions than for
125 biodiesel production.

126 2.4.2. Fatty acid methyl esters (FAMES) and cetane number determination.

127 Biodiesel FAME percentages were calculated following UNE-EN 14103:2011 standard.

128 The percentage of each FAME in the sample was determined by gas chromatography

129 using methyl heptadecanoate as internal standard. An HP 5890 series II gas

130 chromatograph equipped with a SP2380 capillary column (60 m × 0.25 mm internal

131 diameter × 0.25 µm film thickness) was used. The column temperature was set to 185

132 °C and then the temperature program ramped from this temperature to 220 °C at 3 °C

133 min⁻¹. The injection was operated in splitless mode, the injector and detector

134 temperatures being 210 °C and 250 °C, respectively. FAMES were identified by mass

135 spectrometry, comparing the spectra with those in the database for this type of

136 compounds (Wiley, NIST). Additionally, two WCO samples randomly chosen (samples

137 2 and 12) were analysed as well. To analyse these samples, 50 mg of each WCO were

138 dissolved in 2 cm³ heptane and then transesterified using 0.3 cm³ 2 N methanolic

139 potassium hydroxide solution. After decanting, the supernatant was collected and

140 FAME percentages were analysed in the GC system.

141 Cetane number (CN) of biodiesel was calculated from the FAME composition using the

142 equation proposed by Bamgboye and Hansen [6]:

$$143 \text{CN} = 61.1 + 0.088x_2 + 0.133x_3 + 0.152x_4 - 0.101x_5 - 0.039x_6 - 0.243x_7 - 0.395x_8$$

144 where x_2 , x_3 , x_4 , x_5 , x_6 , x_7 and x_8 stand for myristic, palmitic, stearic, palmitoleic, oleic,

145 linoleic and linolenic acid methyl esters percentages (% wt.), respectively. The cetane

146 number ranged between 46.8 and 59.8 (Table 1).

147 2.4.3. VIS/NIR spectra acquisition

148 Prior to spectra acquisition, WCO and biodiesel samples were placed in a thermostatic
149 water bath and maintained at 32 °C for 30 min, since temperature has an important
150 influence on the NIR radiation a sample reflects and absorbs.

151 A Vis/NIR Labspec Pro model LSP 350-2500P (Analytical Spectral Devices Inc.,
152 Boulder, CO, USA) spectrophotometer equipped with three detectors was used for
153 spectral acquisition, as described elsewhere [12]. The instrument is equipped with
154 internal shutters and automatic offset correction, the scanning speed time being 100 ms.
155 The spectrometer was equipped with a spectrophotometric cuvette accessory joined by
156 fibre optic connectors to the light source of the spectrometer on one side, and to the
157 detector of the spectrometer on the opposite side.

158 NIR spectra acquisition from 800 to 2200 nm was carried out in transmittance mode
159 using a 10-mm quartz cuvette with wavelength increment of 1 nm. This optical path
160 length was selected because it showed higher absorption intensity than 1 mm, 2 mm and
161 5 mm path-length quartz cuvettes when acquiring olive oil NIR spectra [12]. The
162 spectra of WCO and biodiesel samples were recorded using the Indico Pro software
163 (Analytical Spectral Devices Inc., Boulder). Two replicas of each sample were acquired.

164 2.4.4. Calibration procedure and model evaluation

165 Reflectance data was first transformed to absorbance. The resulting spectra were
166 divided into calibration and validation sets. Thirty randomly samples were used for
167 multivariable calibration and the 20 remaining samples were used as validation set.
168 Partial least squares (PLS) models using full-cross internal validation were built with
169 The Unscrambler software (CAMO Software AS, Norway).

170 The performance of the models was evaluated based on root mean square error of
171 calibration (RMSEC), root mean square error of full-cross validation (RMSECV),
172 multiple correlation coefficient of calibration (r^2_c) and multiple correlation coefficient of
173 full-cross validation (r^2_{cv}) in the calibration sample set, and root mean square error of
174 prediction (RMSEP), standard error of prediction (SEP) and ratio of performance to
175 deviation (RPD) in the validation sample set. Among them, the most important
176 parameters to assess the performance of the model are r^2_c (calibration) and RPD
177 (validation): the higher these parameters are, the higher the accuracy of the model.

178

179 **3. Results and Discussion**

180 3.1. Features of the WCO and biodiesel NIR spectra

181 NIR absorption is assumed linear with the concentration of organic materials. The NIR
182 spectrum of a sample is composed of the first and second overtones (800-1800 nm) and
183 combinations bands (1800-2700 nm) of fundamental, largely hydrogenic, vibrations that
184 occur in the MIR region. The acquired WCO and biodiesel absorbance spectra are
185 shown in Fig. 1, showing various overlapping peaks. The obtained spectra for WCOs
186 (Fig. 1a) are similar to those previously obtained for olive oils, so their main features
187 are described elsewhere [12]. Briefly, from 800 to 2200 nm, firstly a broad absorbance
188 band occurs at 1210 nm due to C–H second overtones and CH=CH– stretching
189 vibrations. Then, a large, strong absorption band of the water first overtone is found in
190 the range 1350-1450 nm. The absorption intensity near 1720 nm is related to the first
191 overtone of the C–H vibration of several chemical groups (=CH–, –CH₃, –CH₂–).
192 Another broad water combination band is observed at 1880-2100 nm. The two

193 described water bands consist of multiple overlapping bands. Finally, the absorption
194 band of the C–H vibration of *cis*-unsaturation occurs in the area close to 2143 nm.
195 Interestingly, biodiesel NIR spectra were identical to WCO NIR spectra (Fig. 1b).
196 Similarly to WCO spectra, the highest intensity peak in biodiesel spectra was found
197 near 1725 nm, wavelength in which the maximum absorption band of the triolein
198 spectrum has been reported [21]. Obviously, biodiesel does not contain triolein, so this
199 absorption band and the one close to 2143 nm are probably due to the above-mentioned
200 C–H vibrations of the fatty acids of the FAMEs (and therefore of the fatty acids of
201 triglycerides in WCO spectra). Vegetable oils are mainly composed of triglycerides
202 while biodiesel is composed of FAME. Since transesterification reaction (regardless the
203 reactor type and operational conditions) does not alter the fatty acids of triglycerides [4],
204 the fatty acid composition of the starting oil should be the same than the fatty acid
205 composition of the resulting biodiesel [1–3]. Therefore, it can be logical that the NIR
206 spectrum of an oil and that of its derived biodiesel are the same. The solely, slight
207 difference between WCO and biodiesel spectra was found in the range 2150–2200 nm,
208 the absorption intensity being higher in biodiesel spectra.

209 3.2. Free acidity

210 Three WCOs (samples 18, 35 and 42) had FA higher than 2.5 % (Table 1), so these
211 samples were subjected to previous esterification to reduce their acidity. Neither the
212 resulting FAs nor NIR spectra were measured after esterification because these WCOs
213 were immediately subjected to transesterification in the same reactor. NIR spectra
214 corresponding to these 3 samples were, therefore, those acquired for the starting WCOs.

215 3.3. Cetane number results from FAME composition

216 Biodiesel usually has cetane number higher than conventional diesel, providing thus
217 better combustion efficiency. The FAME content is of major importance because the
218 overall fuel properties of a biodiesel sample can be obtained from the properties of the
219 individual fatty acid methyl esters that comprise it [1,3]. Cetane number is one of these
220 properties depending on FAME composition and therefore was calculated from this
221 composition applying the equation proposed by Bamgboye and Hansen [6]. There were
222 noticeable differences in biodiesel FAME composition depending on the type of
223 vegetable oil from which WCO came from (Table 1). On the contrary, there were not
224 differences in FAME composition between starting WCO and resulting biodiesel of the
225 two samples analysed (data not shown), which verifies that transesterification does not
226 alter FAME profile. Thus, the palmitic, stearic, oleic and linoleic acids percentages in
227 biodiesel sample 2 were 13.2, 3.1, 71.7 and 8.2, respectively, while they were 13.1, 3.2,
228 72.0 and 8.4, respectively, in the WCO sample 2.

229 Applying the Bamgboye and Hansen's equation, the cetane number of the 50 biodiesel
230 samples ranged between 46.8 and 59.8 (Table 1), being the standard deviation 4.73. The
231 standard deviation of the validation set (20 samples), required for the calculation of
232 RPD in NIRS, was similar (4.74). Cetane numbers from olive oil-derived biodiesels
233 were markedly higher than those of sunflower oil-derived biodiesels because of the
234 higher content in linoleic acid of sunflower oil. The cetane numbers obtained are higher
235 than those of petroleum diesel fuels (48-51) and are in the range indicated in the UNE-
236 EN 14214:2013 standard for biodiesel derived from vegetable oils, which illustrates the
237 potential of biodiesel fuel from WCO.

238 3.4. Cetane number calculation from biodiesel NIR spectra.

239 FAME determination by NIRS in vegetable oils [14] and biodiesel [15] has been
240 previously reported. Since cetane number was calculated from FAME composition, it is
241 logical to think that cetane number can be also obtained from biodiesel NIR spectrum.

242 The PLS calibration model built using NIR absorbance spectra of the 30 biodiesel
243 samples of the calibration set, without any previous pretreatment or normalization,
244 achieved r^2_c , r^2_{cv} , RMSEC and RMSECV of 0.990, 0.983, 0.470 and 0.621, respectively
245 (Table 2). The number of optimal principal components to build this PLS model was
246 four. According to Shenk *et al.* criteria [22], the PLS calibration model had excellent
247 precision ($r^2_c \geq 0.90$), and the root mean square error was low. The full cross validation
248 statistics confirmed the goodness of the PLS model. This calibration model was used in
249 the prediction exercises. The predicted cetane numbers of the 20 samples of the
250 validation set are listed in Table 1. As can be observed in Table 2, SEP was 1.108,
251 providing $RPD = 4.27$, which accounts for the excellent precision of the obtained PLS
252 model for cetane number determination from biodiesel NIR spectra. According to
253 criteria mentioned earlier [22], RPD must be higher than 3 for a PLS model to be
254 considered of excellent precision. Other author stated that predictive models with RPD
255 values between 2 and 10 are suitable for routine analysis [23]. These results could be
256 improved using normalized or derivative spectra, eliminating spectral variables without
257 information related to the measured parameter, such as noise and background, or
258 eliminating outliers in the calibration and validation sets [12]. However, these
259 techniques were not assayed because it was not the aim of this work. Just as an example,
260 by eliminating sample 37 from the validation set (sample marked by The Unscrambler
261 software as outlier) SEP decreases up to 0.802 and therefore RPD increases to 5.90.

262 3.5. Cetane number prediction from WCO NIR spectra

263 As mentioned earlier, fatty acid composition was not modified by transesterification
264 reaction and WCO and biodiesel spectra were similar. Therefore, biodiesel cetane
265 number could be predicted from the NIR spectrum of the starting WCO. For further
266 comparison with the results obtained with biodiesel spectra, the PLS model for cetane
267 number prediction from WCO NIR spectra was also directly built without any spectrum
268 pretreatment. The calibration statistics are shown in Table 2, showing the excellent
269 performance of the PLS model ($r^2_c = 0.971$; RPD = 3.83), the number of principal
270 components being again equal to four. The performance of cetane number prediction
271 using WCO NIR spectra was somehow lower than when using biodiesel NIR spectra.
272 This could be due to the fact that biodiesel samples are clean (distilled and filtered),
273 being almost exclusively composed of FAME, while WCOs contained not only
274 triglycerides, but also part of the other vegetable oil compounds and different
275 degradation compounds due thermal, oxidative and hydrolytic reactions occurring
276 during frying, as mentioned earlier [17], which can affect the PLS model. The removal
277 of uninformative spectral variables from the PLS calibration model would enhance the
278 prediction performance [12]. Nevertheless, the potential and accuracy of both cetane
279 number calculation from NIR biodiesel spectra and cetane number prediction from
280 starting WCO NIR spectra are demonstrated. SEP using biodiesel and WCOs spectra
281 were 1.108 and 1.238, respectively. Other methods, such the ASTM D4737-10(2016)
282 standard for the calculation of cetane number of distillate fuels from density and
283 distillation recovery temperature measurements, have higher experimental errors. To be
284 specific, this standard ASTM D4737-10(2016) estimates the ASTM cetane number
285 (Test Method D613) of distillate fuels with cetane number within the range from 32.5 to
286 56.5 with an expected error of prediction lower than ± 2 units for 65 % of the distillate
287 fuels, indicating that errors may be even greater for fuels whose properties fall outside

288 the recommended range of application. The repeatability and the reproducibility of this
289 ASTM D613 test method to calculate the cetane number of biodiesel samples from
290 soybean oil have been reported to be ± 0.9 units and ± 4.3 units, respectively [11].

291 What is more, the r^2 of the equation used to calculate cetane number based on biodiesel
292 FAME composition [6], used as reference data in this work, was 0.883, which indicates
293 that this equation can predict cetane number with solely 88 % accuracy. Similar
294 equations that correlate biodiesel cetane number with FAME weight composition can be
295 found in literature [7–9]. A comparative study among these equations using biodiesels
296 from many sources and feedstocks exhibited r^2 values of 0.82, 0.81, 0.80 and 0.83 for
297 the equations of Bamgboye and Hansen [6], Gopinath *et al.* [7], Piloto Rodríguez *et al.*
298 [8] and Giakoumis and Sarakatsanis [9], respectively. The absolute error when
299 predicting cetane number of WCO-derived biodiesel using the Giakoumis and
300 Sarakatsanis' equation was 8.9 % [9].

301 Biodiesel cetane number can be also calculated from the weight percentage of each
302 FAME in the biodiesel sample and the cetane number of each FAME [3,10], percent
303 errors between 1.6 % and 16.3 % being reported for different biodiesel fuels [10]. The
304 cetane number of each FAME can be calculated through an equation based on its
305 molecular weight and its number of double bonds with an average absolute deviation of
306 5.95 % [11]. Some authors have claimed that the biodiesel cetane number prediction
307 errors using this last equation are minor than the previously reported by Bamgboye and
308 Hansen [11].

309 It is worth noting that if FAME composition of a biodiesel and its starting oil are
310 identical (transesterification reaction does not alter FAME profile), biodiesel cetane
311 number could be also predicted by applying any of the aforementioned equations to oil
312 fatty acid composition. However, NIRS is cheaper (not only in terms of equipment, but

313 also considering reagents and maintenance) and much quicker than gas
314 chromatography. Besides, NIRS would allow for real-time determination of cetane
315 number. Therefore, NIRS is more suitable for cetane number prediction than equations
316 based on FAME composition.

317

318 **4. Conclusions**

319 Near infrared spectroscopy showed great potential for the fast and accurate prediction of
320 biodiesel cetane number. NIRS allowed for the determination of cetane number not only
321 from biodiesel NIR spectra, but also from waste cooking oil NIR spectra, reaching high
322 RPD (4.27 and 3.83, respectively), thus demonstrating the accuracy of the PLS models
323 built from NIR spectra. The standard error of prediction of cetane number from waste
324 cooking oil NIR spectra was 1.2, which is in agreement with the errors provided by both
325 the ASTM standard method and the proposed equations based on FAME composition
326 available in literature. This implies that cetane number of a future biodiesel can be
327 predicted prior performing transesterification reaction by acquiring NIR spectrum of the
328 starting oil. The advantages for industrial implementation are, therefore, numerous,
329 because cetane number prediction from NIR oil spectra would allow discarding
330 substrates not suitable for biodiesel production, thus reducing costs. This NIRS
331 prediction is due to the fact that fatty acid distribution of the produced biodiesel and that
332 of its starting oil are the same, and biodiesel cetane number depends on the fatty acid
333 composition (mainly chain length and unsaturation number) of the substrate from which
334 it is produced. NIR spectra of biodiesels and waste cooking oils were alike, probably
335 because they show mostly C–H vibrations of fatty acids.

336

337 **Acknowledgements**

338 This work was supported by the European Union Funds under grant LIFE 13-Bioseville
339 ENV/ES/1113.

340

341 **References**

342 [1] Knothe G. Dependence of biodiesel fuel properties on the structure of fatty acid
343 alkyl esters. *Fuel Process Technol* 2005;86:1059–70.

344 doi:10.1016/j.fuproc.2004.11.002.

345 [2] Giwa SO, Adama KO, Nwaokocha CN, Solana OI. Characterization and flow
346 behaviour of sandbox (*Hura crepitans* Linn) seed oil and its methyl esters. *Int*
347 *Energy J* 2016;16:65–72.

348 [3] Ramos MJ, Fernández CM, Casas A, Rodríguez L, Pérez Á. Influence of fatty
349 acid composition of raw materials on biodiesel properties. *Bioresour Technol*
350 2009;100:261–8. doi:10.1016/j.biortech.2008.06.039.

351 [4] García-Martín JF, Barrios CC, Alés-Álvarez FJ, Dominguez-Sáez A, Alvarez-
352 Mateos P. Biodiesel production from waste cooking oil in an oscillatory flow
353 reactor. Performance as a fuel on a TDI diesel engine. *Renew Energy*
354 2018;125:546–56. doi:10.1016/j.renene.2018.03.002.

355 [5] Xiao G, Gao L. First Generation Biodiesel. *Biofuel Prod - Recent Dev Prospect*
356 2010:45–64.

357 [6] Bangboye AI, Hansen AC. Prediction of cetane number of biodiesel fuel from
358 the fatty acid methyl ester (FAME) composition. *Int Agrophysics* 2008;22:21–9.

- 359 [7] Gopinath A, Puhan S, Nagarajan G. Relating the cetane number of biodiesel fuels
360 to their fatty acid composition: A critical study. *Proc Inst Mech Eng Part D J*
361 *Automob Eng* 2009;223:565–683. doi:10.1243/09544070JAUTO950.
- 362 [8] Piloto-Rodríguez R, Sánchez-Borroto Y, Lapuerta M, Goyos-Pérez L, Verhelst S.
363 Prediction of the cetane number of biodiesel using artificial neural networks and
364 multiple linear regression. *Energy Convers Manag* 2013;65:255–61.
365 doi:10.1016/j.enconman.2012.07.023.
- 366 [9] Giakoumis EG, Sarakatsanis CK. Estimation of biodiesel cetane number, density,
367 kinematic viscosity and heating values from its fatty acid weight composition.
368 *Fuel* 2018;222:574–85. doi:10.1016/j.fuel.2018.02.187.
- 369 [10] Clements LD. Blending rules for formulating biodiesel fuel, in liquid fuels and
370 industrial products from renewable resources. *Proc. third Liq. fuel Conf.*
371 Nashville, TN, 1996, p. 44–53.
- 372 [11] Ramírez-Verduzco LF, Rodríguez-Rodríguez JE, Jaramillo-Jacob ADR.
373 Predicting cetane number, kinematic viscosity, density and higher heating value
374 of biodiesel from its fatty acid methyl ester composition. *Fuel* 2012;91:102–11.
375 doi:10.1016/j.fuel.2011.06.070.
- 376 [12] García Martín JF. Optical path length and wavelength selection using Vis/NIR
377 spectroscopy for olive oil's free acidity determination. *Int J Food Sci Technol*
378 2015;50:1461–7. doi:10.1111/ijfs.12790.
- 379 [13] Zhang WB. Review on analysis of biodiesel with infrared spectroscopy. *Renew*
380 *Sustain Energy Rev* 2012;16:6048–58. doi:10.1016/j.rser.2012.07.003.
- 381 [14] Marquez AJ, Díaz AM, Reguera MIP. Using optical NIR sensor for on-line

- 382 virgin olive oils characterization. *Sensors Actuators, B Chem.*, vol. 107, 2005, p.
383 64–8. doi:10.1016/j.snb.2004.11.103.
- 384 [15] Baptista P, Felizardo P, Menezes JC, Correia MJN. Multivariate near infrared
385 spectroscopy models for predicting the methyl esters content in biodiesel. *Anal*
386 *Chim Acta* 2008;607:153–9. doi:10.1016/j.aca.2007.11.044.
- 387 [16] Mittelbach M, Enzelsberger H. Transesterification of heated rapeseed oil for
388 extending diesel fuel. *J Am Oil Chem Soc* 1999;76:545–50. doi:10.1007/s11746-
389 999-0002-x.
- 390 [17] Nawar WW. Chemical Changes in Lipids Produced by Thermal Processing. *J*
391 *Chem Educ* 1984;61:299–302. doi:10.1021/ed061p299.
- 392 [18] Cvengroš J, Cvengrošová Z. Used frying oils and fats and their utilization in the
393 production of methyl esters of higher fatty acids. *Biomass and Bioenergy*
394 2004;27:173–81. doi:10.1016/j.biombioe.2003.11.006.
- 395 [19] EU standard methods. Commission Regulation (EEC) No 2568/91 on the
396 characteristics of olive oil and olive-residue oil and on the relevant methods of
397 analysis. *Off J Eur Communities* 1991:1–15. doi:2004R0726 - v.7 of 05.06.2013.
- 398 [20] European Union. COMMISSION IMPLEMENTING REGULATION (EU) No
399 1348/2013 amending Regulation (EEC) No 2568/91. *Off J Eur Union*
400 2013;2013:31–67.
- 401 [21] García-González DL, Baeten V, Fernández Pierna JA, Tena N. Infrared, raman,
402 and fluorescence spectroscopies: Methodologies and applications. *Handb. Olive*
403 *Oil Anal. Prop.*, 2013, p. 335–93. doi:10.1007/978-1-4614-7777-8_10.
- 404 [22] Shenk JS, Workman JJ, Westerhans MO. Application of NIRS to agricultural

405 products. *Handb Near-Infrared Anal* 1992:383–431.

406 doi:doi:10.1201/9781420002577.pt4a.

407 [23] Fearn T. Assessing calibrations: SEP, RPD, RER and R2. *NIR News*

408 2002;13:12–3. doi:10.1255/nirn.689.

409

Table 1

Table 1. Free acidity (FA) of starting WCO, biodiesel FAME composition, cetane number of the produced biodiesels calculated by Bamgboye and Hansen equation (CN FAME) and biodiesel NIR spectra (CN Fuel-NIR), predicted cetane numbers using WCO NIR spectra (CN Oil-NIR) and type of vegetable oil used to produce WCO.

Sample	FA (%)	14:0 (%)	16:0 (%)	16:1 (%)	18:0 (%)	18:1 (%)	18:2 (%)	18:3 (%)	CN FAME	CN Fuel-NIR	CN Oil-NIR	Starting WCO
1	0.21	0.24	7.8	3.1	0.23	30.4	55.0	0.12	48.0			Sunflower
2	0.60	0.08	13.2	3.1	1.19	71.7	8.2	0.14	58.4			Olive
3	1.61	0.00	12.7	3.6	0.75	71.8	6.8	0.15	58.7			Olive
4	2.17	0.08	8.2	3.3	0.35	33.1	53.2	0.12	48.4			Sunflower
5	2.01	0.00	13.7	3.7	0.67	75.9	2.5	0.12	59.8			Olive
6	0.29	0.03	13.5	3.9	0.09	74.5	6.2	0.17	59.0			Olive
7	1.30	0.17	14.3	3.2	0.00	72.8	5.8	0.15	59.2			Mixture
8	0.67	0.03	14.4	3.2	0.00	74.1	5.7	0.19	59.2			Mixture
9	1.10	0.14	14.3	3.1	0.00	72.8	6.0	0.13	59.1			Mixture
10	1.16	0.13	13.9	2.8	0.00	74.0	5.3	0.16	59.1			Olive
11	0.62	0.09	14.6	3.1	0.00	73.5	5.6	0.15	59.2			Olive
12	1.22	0.17	14.5	3.0	0.00	73.5	5.8	0.39	59.1			Olive
13	0.50	0.03	14.5	2.5	0.00	70.3	7.3	0.13	58.9			Olive
14	0.24	0.06	7.6	2.9	0.13	36.8	49.2	0.09	49.1			Sunflower
15	0.66	0.08	9.9	3.5	0.14	73.2	10.6	0.19	57.4			Mixture
16	0.41	0.07	7.5	2.6	0.12	29.0	59.5	0.16	46.8			Sunflower
17	0.69	0.05	13.0	3.4	0.07	73.9	6.3	0.16	58.9			Olive
18	9.72	0.13	8.5	3.2	0.17	35.3	50.6	0.20	49.0			Mixture
19	0.94	0.20	14.2	3.2	0.00	44.0	34.6	0.15	53.3			Mixture
20	0.33	0.14	7.8	3.2	0.24	30.8	53.4	0.08	48.4			Sunflower

21	0.52	0.15	14.6	3.8	0.13	72.3	5.5	0.15	59.4			Olive
22	0.15	0.03	13.6	3.8	0.06	74.8	4.6	0.17	59.4			Olive
23	0.72	0.09	12.6	3.9	0.08	61.7	19.9	0.19	56.1			Mixture
24	0.24	0.13	8.1	3.4	0.00	31.3	52.8	0.09	48.6			Sunflower
25	0.21	0.17	7.6	3.1	0.00	29.5	57.0	0.08	47.6			Sunflower
26	0.88	0.06	13.2	3.3	0.93	71.7	4.6	0.34	59.2			Mixture
27	1.91	0.12	12.2	3.2	0.85	64.0	17.2	0.17	56.4			Mixture
28	1.21	0.08	13.0	3.0	0.96	66.4	13.7	0.17	57.2			Mixture
29	0.21	0.00	12.2	3.6	0.88	73.6	7.4	0.19	58.4			Olive
30	0.50	0.06	11.6	3.2	0.89	66.9	12.3	0.17	57.4			Olive
31	0.37	0.13	8.4	3.5	0.27	34.5	50.5	0.14	49.1	49.2	49.8	Sunflower
32	1.28	0.02	11.3	3.7	0.61	74.5	4.7	0.19	59.0	60.4	58.9	Olive
33	1.29	0.00	11.5	3.6	0.66	74.9	4.5	0.17	59.0	60.0	58.6	Olive
34	0.71	0.09	13.0	2.7	1.10	67.9	12.6	0.20	57.4	58.0	57.8	Olive
35	3.33	0.16	13.9	3.2	0.90	72.9	5.3	0.19	59.2	60.1	57.6	Olive
36	1.06	0.06	13.7	3.1	0.82	68.0	12.8	0.22	57.5	59.0	59.7	Pomace
37	1.05	0.06	13.9	2.6	0.68	69.1	10.7	0.19	57.9	62.5	59.1	Pomace
38	0.37	0.14	8.0	3.0	0.22	38.7	47.8	0.10	49.4	49.7	48.5	Sunflower
39	0.22	0.35	8.5	3.1	0.35	46.6	39.2	0.12	51.3	52.2	50.8	Sunflower
40	0.30	0.12	7.6	3.1	0.34	31.2	55.4	0.13	47.8	48.2	47.5	Mixture
41	2.22	0.04	13.3	3.5	0.91	74.9	5.0	0.21	59.1	60.4	58.4	Olive
42	3.37	0.13	13.8	3.9	0.97	74.2	4.7	0.13	59.4	62.3	58.1	Olive
43	0.98	0.10	7.7	3.8	0.12	31.5	55.6	0.10	47.9	50.8	48.7	Olive
44	0.65	0.05	10.6	3.4	0.61	62.7	21.6	0.15	55.2	56.1	57.2	Olive
45	0.21	0.08	7.2	3.1	0.13	31.4	55.9	0.09	47.7	48.5	46.5	Sunflower
46	0.28	0.15	8.3	3.0	0.31	34.5	51.3	0.09	48.8	49.6	50.5	Sunflower
47	0.61	0.05	9.4	2.9	0.56	74.3	10.5	0.19	57.2	57.8	58.8	Mixture
48	0.58	0.08	8.1	3.2	0.28	34.8	52.7	0.13	48.4	48.8	50.1	Sunflower

49	1.03	0.06	11.6	3.0	0.68	58.3	25.0	0.16	54.6	56.8	54.1	Mixture
50	2.30	0.17	13.2	4.3	1.26	69.2	9.2	0.15	58.4	58.7	58.8	Olive

14:0 = myristic acid; 16:0 = palmitic acid; 18:0 = stearic acid; 16:1 = palmitoleic acid; 18:1 = oleic acid; 18:2 = linoleic acid; 18:3 = linolenic acid.

Table 2. Calibration and prediction statistics for cetane number calculation using biodiesel and WCO spectra.

	r^2_c	r^2_{cv}	RMSEC	RMSECV	RMSEP	SEP	RPD
CN Fuel-NIR	0.990	0.983	0.470	0.621	1.650	1.108	4.27
CN Oil-NIR	0.971	0.965	0.760	0.867	1.260	1.238	3.83

r^2_c : correlation coefficient of calibration; r^2_{cv} : correlation coefficient of full cross validation;

RMSEC: root mean square error of calibration; RMSECV: root mean square error of full cross validation; RMSEP: root mean square error of prediction; SEP: standard error of prediction;

RPD: ratio of performance to deviation.

Figure 1

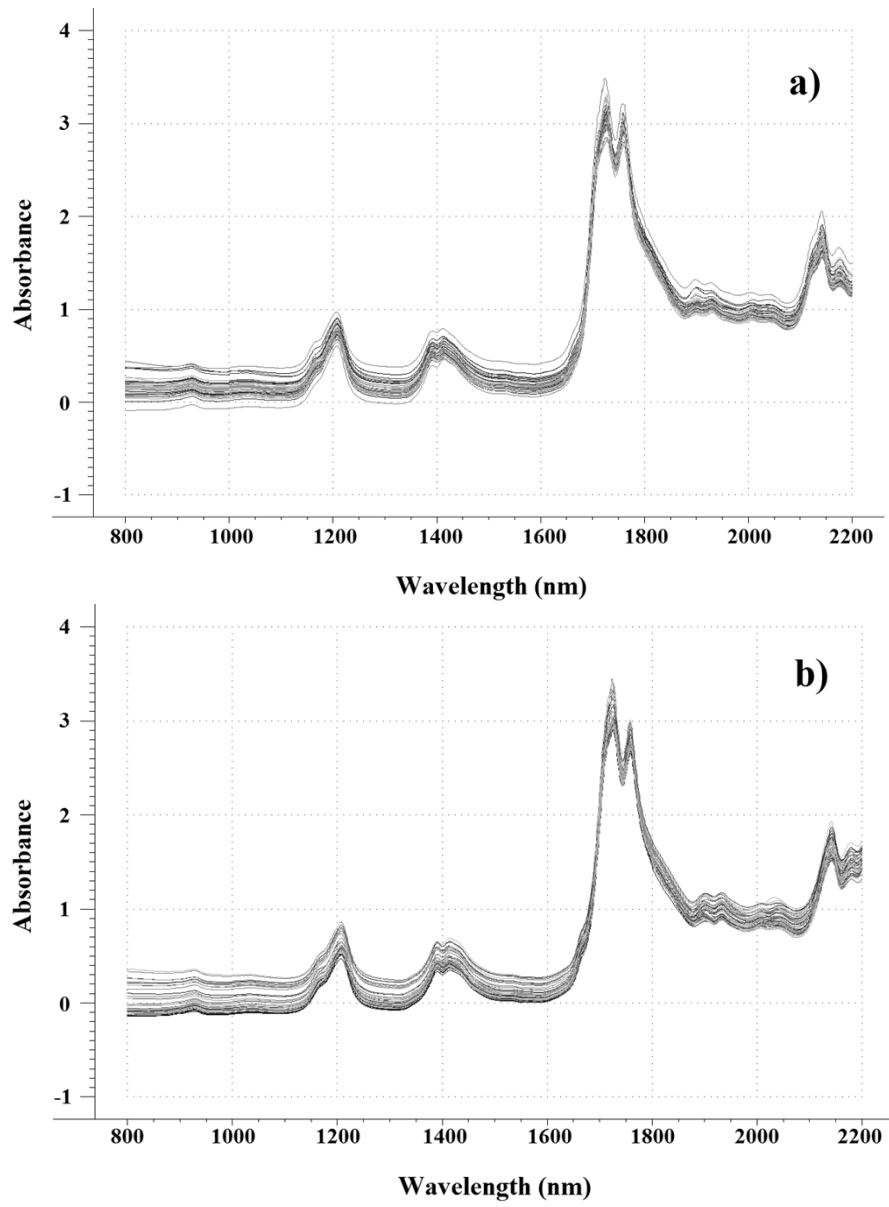


Fig. 1. WCO (a) and biodiesel (b) NIR spectra.